SSC19-WKV-05

The Low-Latitude Ionosphere/Thermosphere Enhancements in Density (LLITED) Mission

Rebecca L. Bishop, Richard Walterscheid
The Aerospace Corporation
El Segundo, CA 90245; (310) 336-1750
Rebecca.L.Bishop@aero.org

James Clemmons
University of New Hampshire
Durham, NH 03824 (603) 862-2465
James.Clemmons@unh.edu

Aroh Barjatya, Liam O. Gunter
Embry-Riddle Aeronautical University
Daytona Beach, FL, 32114; (386) 226-6675
barjatya@erau.edu

ABSTRACT

The Low-Latitude Ionosphere/Thermosphere Enhancements in Density (LLITED) CubeSat mission is a NASA funded HTIDs project. It is a 3-year grant with two 1.5U CubeSats with an estimated delivery in the spring of 2020 and a 1-year on-orbit mission life. Each CubeSat will host a miniature ionization gauge space instrument (MIGSI), planar ion probe (PIP), and GPS radio occultation sensor (CTECS-A). The mission is to provide both ionosphere and thermosphere measurements related to the Equatorial Ionization Anomaly (EIA) and the Equatorial Temperature and Wind Anomaly (ETWA). The EIA and ETWA are two of the dominant ionosphere/thermosphere interactions on the low-latitude duskside. While the EIA has been extensively studied both observationally and with modeling, the ETWA is less well known since observations are infrequent due to a lack of suitably instrumented spacecraft (s/c) at appropriate altitudes. LLITED will, for the first time, provide coincident high-resolution measurements of the duskside ionosphere/thermosphere at lower altitudes that will characterize and improve our understanding of the ETWA, provide insight into the coupling physics between the ETWA and EIA, and increase our knowledge of the duskside dynamics that may influence space weather. The following paper reviews the science mission and concepts and then provides the current status of the LLITED hardware.

INTRODUCTION

Recent observations of the duskside thermosphere have revealed additional complexity to the coupling between the ionosphere/thermosphere (IT) regions and its potential impact on space weather. There exist two dominant IT interactions in the low-latitude dusks-side: the Equatorial Ionization Anomaly (EIA) and the Equatorial Temperature and Wind Anomaly (ETWA). While the EIA has been extensively studied both observationally and with modeling, the ETWA is less well known since observations are infrequent due to a lack of suitably instrumented spacecraft (s/c) at appropriate altitudes. The Low-Latitude Ionosphere/Thermosphere Enhancements in Density (LLITED) CubeSat mission proposes to provide both ionosphere and thermosphere measurements that will be used to characterize and improve our understanding of the ETWA, provide insight into the coupling physics between the ETWA and EIA, and increase our knowledge of the duskside dynamics that may influence space weather. For the first time, coincident high-resolution measurements of the duskside thermosphere/ionosphere at lower altitudes will be made, providing a detailed examination of the ETWA.

The mission will consist of two 1.5U (10 x 10 x 15 cm) CubeSats in a high-inclination circular orbit, with an orbit altitude requested between 350 and 450 km. The CubeSats will maintain a 1/4 to 1/2 orbit separation to each other in order to observe any temporal changes as the ETWA evolves. Both CubeSats will host three payloads: an ionization gauge (IG), planar ion probe (PIP), and GPS radio occultation sensor (GPSRO). The products provided are in-situ neutral pressure/density, in-situ plasma density, and slant TEC. The observations from LLITED will be combined with other available data, such as the remote sensing observations of ICON, to provide a comprehensive dataset of the ETWA.

ETWA AND EIA

The low latitude nighttime IT region (100-500km) contains large scale features and a host of phenomena including space weather driven events such as Equatorial Spread-F and scintillation. Two prominent features of the region are the Equatorial Ionization Anomaly (EIA) and the Equatorial Temperature and Wind (ETWA), which occur to some extent in all longitudes within $\pm$40° geographic latitude.

The EIA consists of regions of enhanced plasma density on either side of the equator and were first discovered by *Namba and Maeda*.[1] Over time the EIA has been extensively studied using observations from a varied array of platforms ranging from ground-based ionosonde and GPS data, to on-orbit in-situ plasma sensors and remote sensing sensors such as FUV imagers and GPS radio occultation.[2,3,4] The formation of the EIA occurs when plasma at the equator is driven upward via the vertical ExB drift, and then diffuses to lower altitudes along geomagnetic field lines. This is also known as the "fountain effect". The variability of the EIA, especially during geomagnetic activity, may provide conditions conducive to various space weather events.

The ETWA is identified by enhancements in the thermospheric neutral temperature and neutral densities that while occurring at low latitudes, also occur at latitudes slightly higher than the EIA. Neutral density enhancements and troughs were originally observed using sensor data from OVE-6 and DE-2 satellites.[5,6] Unlike the EIA, the ETWA is less understood and observations are relatively scarce.

Over the years, a number of studies have proposed mechanisms to explain the formation of the ETWA. The first hypothesis describing ETWA daytime formation involved variations in the zonal ion drag as a function of latitude. This variation results in energy flow from the dayside to the nightside being damped at EIA crest latitudes producing enhancements in neutral temperature and density.[7] Another theory put forth by *Fuller-Rowell et al.* speculated that the ETWA was the result of chemical heating from the exothermic recombination of O+.[8] This theory was tested with model simulations with mixed success.[8,9] The simulations were able to reproduce the vertical wind values coincident with DE-2 observations but was unable to explain the latitude separation or longitudinal variations between the EIA and ETWA phenomena. Other studies explained the appearance of daytime ETWA as the result of tidal coupling.[10,11] None of the studies previously mentioned were able to fully describe the characteristics of the ETWA and its relationship to the EIA.

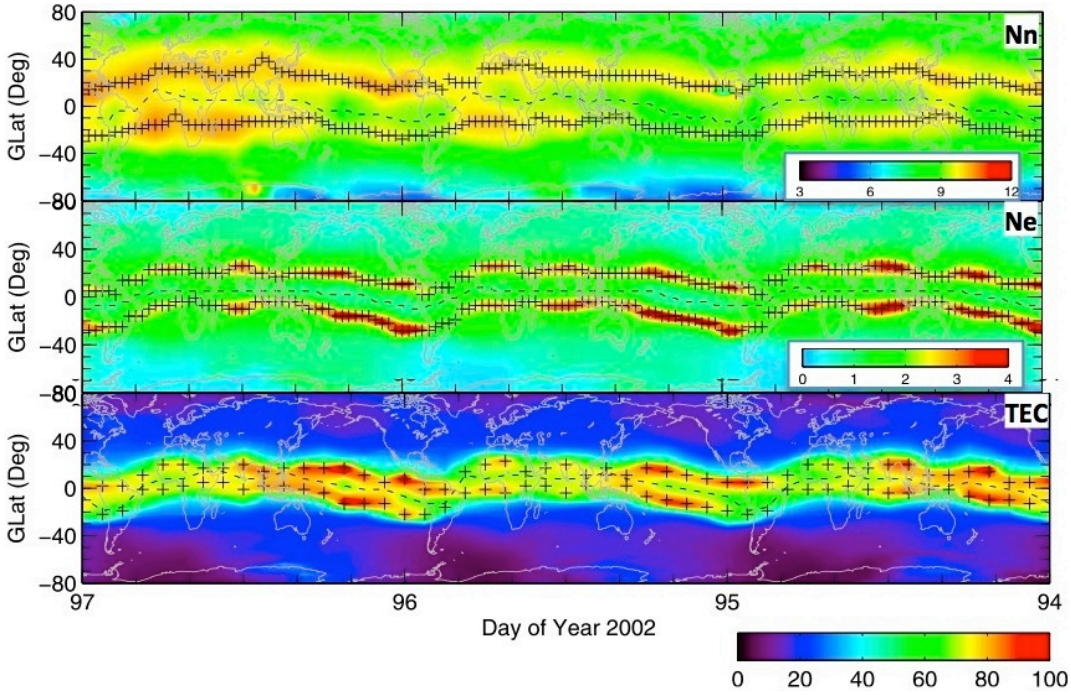

Figure 1: Data from the CHAMP accelerometer (top panel; 10^{-12} kg/m^3), planar Langmuir probe (middle panel; 10^{12} m^{-3}), GPS RO sensor (bottom panel; TECU). Crosses & dashes mark the location of crests & trough, respectively. [adapted from Figures 1, 3, 6 of *Lei et al.* [2010].

More recently, global circulation models have been employed to study the formation and evolution processes of the ETWA.[12,11,13,14,15] *Lei et al.* used the NCAR-TIEGCM model in their study.[16] Multiple simulations revealed that neither zonal winds producing heat transport nor chemical heating due to recombination are capable of explaining the formation of the temperature crests of the ETWA. They concluded that the temperature crests form due to plasma-neutral heating where energy is transferred from thermal electrons and ions to neutrals via collisions. The results showed the crests 10°-15° poleward of the EIA crests. A companion study also using the TIEGCM concluded that the primary mechanism for trough formation is field-aligned ion drag, different from the mechanism for crest formation.[11] Most recently, *Hsu et al.* used the TIEGCM model to study the behavior of the ETWA trough region as a function of local time and solar cycle variations.[15] They found that the inclusion of field-aligned ion drag in the TIEGCM simulation produced a trough at the equator in neutral density and neutral temperature. This inclusion results in plasma-neutral interactions leading to a series of hydrodynamic processes.

Simulations have also been used to study the relationship between the EIA and ETWA. In 2014, *Lei et al.* expanded their original 2012 study to focus on the tidal influences and geomagnetic activity.[14,16] Their studies clearly showed the impact of tidal input on the structure of the two phenomena. Both the EIA and ETWA displayed a zonal wave structure when only migrating tides are specified on the lower boundary. Additionally, a zonal wave-4 structure in both the EIA and ETWA was primarily associated with nonmigrating tides with a minor contribution due to ion-neutral coupling.

The observational studies mentioned above rely on older, limited datasets such as DE-2 and AE-E. More recent studies by *Lei et al.* and *Luan et al.* utilized the data from sensors on the CHAMP and COSMIC satellites, respectively.[17,18] The COSMIC mission, a constellation of six satellites each with a GPS radio occultation receiver, provided between 2000-3000 occultations (slant TEC) per day between 2007-2012. This data provides reasonable global coverage of the ionosphere for average periods of a day or more. *Luan et al.* found that EIA was clearly identifiable throughout the day/night in the TEC data.[18] The CHAMP satellite, launched in 2000, has a nearly circular orbit at 454 km and 87° inclination. The *Lei et al.* utilized data from the CHAMP accelerometer, GPS radio occultation sensor, and Planar Langmuir Probe (PLP).[17] Figure 1 shows data from all three sensors over a three-day period in 2002. The accelerometer data in the top panel was obtained by utilizing a model to derive a scale height for each measurement, then the scale height was used to scale the measurements to a common reference altitude (400 km in Figure 1). This study presented the most complete currently available data set of coincidental geophysical parameters for the EIA and ETWA. The data clearly shows a pair of crests on either side of the magnetic equator for both phenomena. The location of the equatorial trough appears to be in relatively good agreement and roughly follows the geomagnetic equator. The ETWA crests are poleward of the EIA crests as suggested by the simulation results by *Lei et al.*.[14] The data also shows variations in the day-to-day ETWA peak crest values that are not reflected in the EIA. The EIA also shows a clear wave-4 structure that is not seen in the ETWA data, providing further indication that the coupling between the two phenomenon is a complex combination of mechanisms.

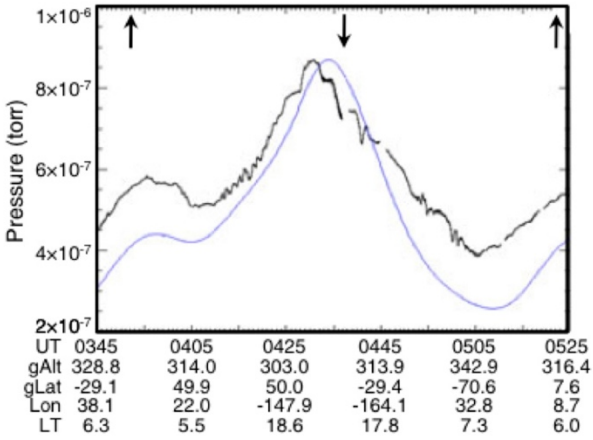

Figure 2: A single orbit of observations from the IG on STREAK (black) with a profile from the MSISE00 model (blue) [from *Clemmons et al.*, 2013].

Finally, the STREAK satellite mission, in orbit 10 months during 2005-2006, hosted an Ionization Gauge Sensor (IGS) that provided a unique data set related to the ETWA. The IGS sampled the sensor's accommodation chamber at a rate of 20 samples for all orbit altitudes (123-350 km). Figure 2 shows a single orbit of IGS data obtained early in the mission.[19] It is customary for densities recorded by ionization gauges to be reported as equivalent pressure at a reference temperature. The data is plotted as a function of UT along with the predictions of the MSISE00 model for reference.[20] Both the IGS and model data show a large-scale structure that is primarily due to the oblateness of the earth resulting in a lower s/c altitude over the equator and thus, higher observed pressures than those observed at higher latitudes. The data also show significant structure on smaller scales, including strong wavelike

features (~100 km) in the high latitude regions and the mesoscale structures evident at lower latitudes.

Both of these wavelike structures are a unique feature of the IGS ETWA observations and illustrate the complex dynamical nature of the phenomenon. *Clemmons et al.* focused on the mesoscale features with a comprehensive examination of the 10-month IGS data set.[20] Figure 3 shows 20 days of filtered measurements from dusk passes with the color scale indicating the level of relative pressure perturbation along each orbital track. While Figure 3 shows crests on either side of the geomagnetic equator similar to earlier observations, there appears to be a second trough poleward of the crests. The crests/troughs have magnitudes approximately 10% of the background. Another interesting feature is the asymmetry of the structure between the northern and southern hemisphere. The ETWA is clearly defined in the northern hemisphere and since the data was obtained near the December solstice, it is likely that the dayside to nightside flow of energy influenced its formation.

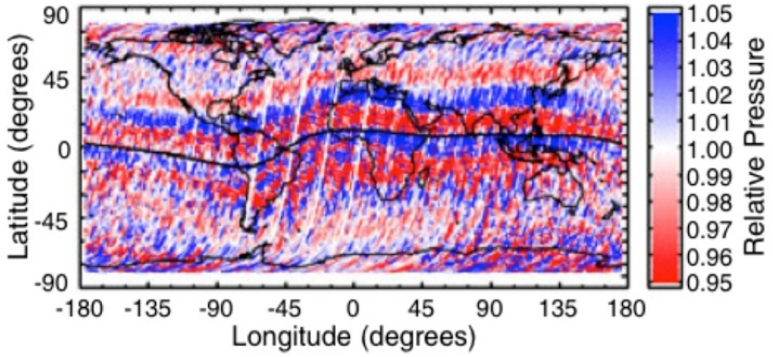

Figure 3: Duskside IGS data from 20days (about 320 spacecraft orbits) near the December solstice of 2005 [from *Clemmons et al.*, 2013].

While the STREAK mission provided highly sensitive measurements of thermospheric pressure via the IGS, it did not include a payload to measure the coincident ionospheric density. However, the GUVI imager on the TIMED mission was operational during the STREAK mission and was oriented during the period shown in Figure 3 such that it imaged local times about one hour after sunset. GUVI provides images of the nightside 135.6 nm emission resulting primarily from the radiant recombination between O+ and electrons in the ionosphere.[21] Figure 4 shows a single day, 14 Oct 2005, of combined IGS and GUVI measurements. The GUVI data clearly displays the low latitude crest and equatorial trough in ionospheric density indicative of the EIA. The overlay of the IGS data shows that ETWA crests and troughs are displaced in latitude from those of the EIA. Figure 4 also shows additional crests/troughs at higher latitudes. In the northern latitudes, up to three troughs and two crests are observed in the IGS in the -180° to -90° longitude range. A similar feature is also observed in the southern hemisphere between ±45° longitude. On the surface, these multiple crest/trough bands appear to be unique to the IGS data set.

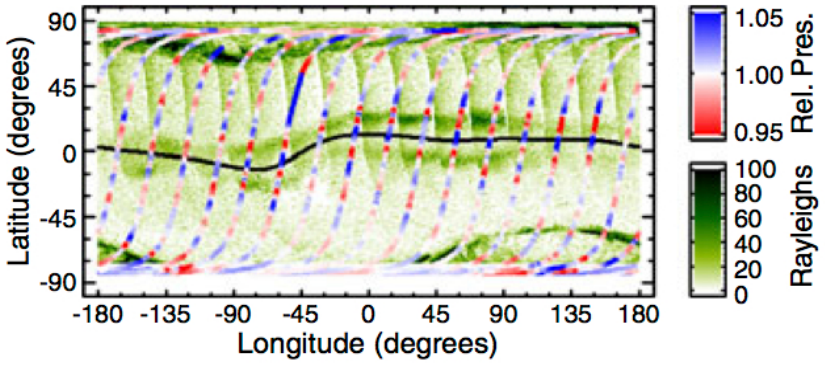

Figure 4: One day (14 October 2005) of measurements of IGS data superposed on data from the GUVI imager on the TIMED spacecraft [from *Clemmons et al.*, 2013].

Because STREAK was in a polar orbit, the IGS was sensitive to changes in the meridional winds. Above 275 km the IGS observed a latitudinal structure in the meridional winds with magnitudes exceeding 300 m/s. The observed latitudinal structure led *Clemmons et al.* to hypothesize that the multiple crest/troughs observed in the pressure data were the result of circulation cells driven by heating in the EIA crests.[20] Figure 5 illustrates a hypothesized mechanism where heated gas under the EIA enhances the neutral pressure in those regions, as observed in the earlier DE-2 measurements, producing pressure gradients to drive the meridional flow. The meridional flow is directed both equatorward and poleward away from the pressure maxima. The equatorward flow must close, so the downwelling, again observed by earlier DE-2 measurements, is the result of continuity and cooling. The explanation for the region between the two pressure maxima described above is the same as presented by *Raghavarao et al.*.[22] The poleward meridional flow from the area under the EIA produces the higher latitude convection cells shown in Figure 5. These cells then drive even weaker higher latitude convection cells through viscous coupling in the downwelling region between the cells. Thus, the four circulation cells centered about the equator are directly driven by the pressure gradients and the cells at higher latitudes are viscously coupled.

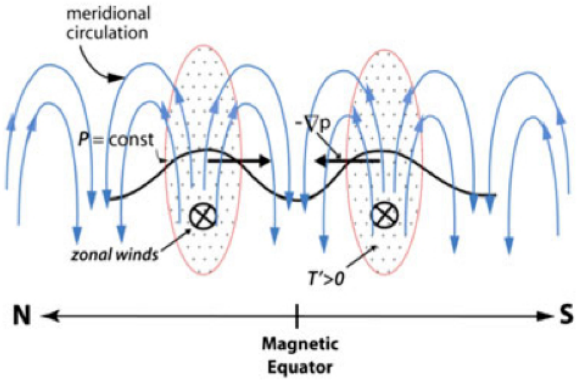

Figure 5: A latitudinal profile illustration of the potential mechanism responsible for the multiple crests/troughs observed by the IGS [from *Clemmons et al.*].[19]

LLITED MISSION

Mission Objectives

While complete understanding of the formation of the ETWA and the coupling mechanisms between it and the EIA is the science community's overall goal in studying these phenomena, it is not one that can be achieved with the currently available datasets. A comprehensive study requires a long-term database (greater than a year) of measurements that include neutral density, wind, and temperature, and plasma density and drift. However, progress can be achieved in understanding this compelling region including specific aspects of the ETWA and its coupling to the EIA. *Clemmons et al.* revealed several new ETWA features including multiple density crests and troughs on either side of the equator (Figure 4) as well as small-scale variations ~100-1000 km (Figure 2) which may in turn be important for the formation of localized space weather events.[19] While the unique IGS dataset dataset contains features not previously seen, a major limitation of the STREAK mission was the lack of in-situ plasma measurements. The LLITED mission will improve on the STREAK mission by providing both in-situ high resolution neutral and plasma density measurements along with the general state of the nearby background ionospheric plasma.

The overall objective of LLITED is to improve our understanding of the relationship between the nightside EIA and ETWA. The specific science questions to be addressed are:

1. What is the mesoscale variability of the ETWA as a function of season, and lon/lat as well as its relationship to EIA heating?
2. What is the relationship between neutral winds (i.e., tides) and the EIA zonal structure?
3. Are the small-scale wave fluctuations in neutral atmosphere quantities, such as those observed by earlier missions exhibited in the ionospheric density?

Table 1 shows the traceability of the three science objectives to the mission capabilities. The LLITED CubeSat Mission is well-positioned to significantly improve our understanding of the compelling EIA/ETWA dynamics, which is important to improving our understanding of conditions that may influence subsequent space weather events. While providing neutral and plasma density measurements, the LLITED mission will overlap with ICON and COSMIC-2 (according to current schedules). These missions will measure plasma densities and drifts, and neutral winds and temperatures. By utilizing all of these datasets, we will be able to construct the most comprehensive picture of EIA/ETWA dynamics to date.

Table 1: Science Traceability Matrix

General Observational Approach	Science Measurement Requirements	Instrument Performance	Limiting Space Systems Requirements
1. Determine the mesoscale variability of the ETWA as a function of season and latitude/longitude as well as its relationship to EIA heating?			
Observations in the 17:00 to 00:00 LT (dusk) sector and over -40° to 55° latitude LLITED Products: In-situ neutral pressure Measurements range: 350– 450 km	In-situ neutral pressure 200 km resolution 2 x 10^{-7} to 1x 10^{-6} torr	MIGSI: Ionization Gauge 1 Hz sampling (8 km) 2 x 10^{-8} to 1x 10^{-2} torr	Orbit: Polar, 350-450km, Circular (preferably 400km) Attitude: 3-axis stabilized Control: 1° Knowledge: 0.1° On-board Data Storage: >8 MB for MIGSI
2. What is the relationship between neutral winds (i.e. tides) and the EIA structure?			
Observations in the 15:00 to 01:00 LT (dusk) sector and over -40° to 55° latitude LLITED Product: Background ionosphere density measurements LLITED Product: Coincident neutral pressure/plasma density Measurements range: 350– 450 km	In-situ neutral pressure: 200 km resolution 2 x 10^{-7} to 1x 10^{-6} torr Plasma Density Profiles: TEC from 100 to 400 km Plasma Density in-track 200 km resolution 10^{12} to 6x10^{12} m^{-3}	MIGSI: Ionization Gauge: 1 Hz sampling (8 km) 2 x 10^{-8} to 1x 10^{-2} torr CTECS-A: GPS RO TEC from 100 to s/c alt. PIP: Planar Ion Probe 1 Hz (~8 km res.) 2x10^{9} to 2x10^{13} m^{-3}	Orbit: Polar, 350-450km, Circular (preferably 400km) Attitude: 3-axis stabilized Control: 1° Knowledge: 0.1° On-board Data Storage: >16 MB for 2 sensors
3. Are the small-scale wave fluctuations in neutral atmosphere quantities, such as those observed by earlier missions exhibited in the ionospheric density?			
Observations in the 15:00 to 01:00 LT (dusk) sector and over -40° to 55° latitude LLITED Product: Coincident neutral pressure/plasma density Measurements range: 350– 450 km	In-situ neutral pressure: 15 km resolution 15 km resolution Plasma Density in-track 200 km resolution 10^{12} to 6x10^{12} m^{-3}	MIGSI: Ionization Gauge 1 Hz sampling (8 km) 2 x 10^{-8} to 1x 10^{-2} torr PIP: Planar Ion Probe 1 Hz (~8 km res.) 2x10^{9} to 2x10^{13} m^{-3}	Orbit: Polar, 350-450km, Circular (preferably 400km) Attitude: 3-axis stabilized Control: 1° Knowledge: 0.1° On-board Data Storage: >128 MB for 3 sensors

LLITED Spacecraft

The Aerospace Corporation xLab Small Satellite department (formerly the PICOSAT group) has participated in the miniature satellite community since its beginning. Starting in 1998, SSDO has designed, fabricated, tested, and flew 8 nanosats. Since 2006, the group has built and launched 24 CubeSats as part of 14 missions with four more mission currently in development. At this moment there are 18 CubeSats operating successfully in orbit with eight in active operations and the remainder in minimal monitoring mode. Each new CubeSat bus has built upon the capabilities of the former resulting in very mature subsystems.

The LLITED mission consists of two 1.5U CubeSats. The LLITED bus structure is similar to AeroCube-7 (launched in August 2016) but with four deployed solar panels instead of two. The subsystem electronics utilizes the majority of AeroCube-10 designs with minor modifications (i.e. white wire corrections). The exception is a payload interface board as well as a high voltage daughter board that is designed specifically for LLITED. Each spacecraft will host the Miniature Ionization Gauge Space Instrument (MIGSI), Planar Ion Probe (PIP), and the Compact Total Electron Content Sensor – Aerospace (CTECS-A).

Figure 6 shows three different views of the current and nearly final CAD model. Adequate space is available for the bus subsystems and payloads as illustrated in

panel A). Panel B) shows the s/c configuration as stowed in the P-pod launcher and immediately upon release. Panel C) illustrates the nominal operational configuration. In each of the panels, the top face contains the MIGSI and planar probe which will be directed into the ram.

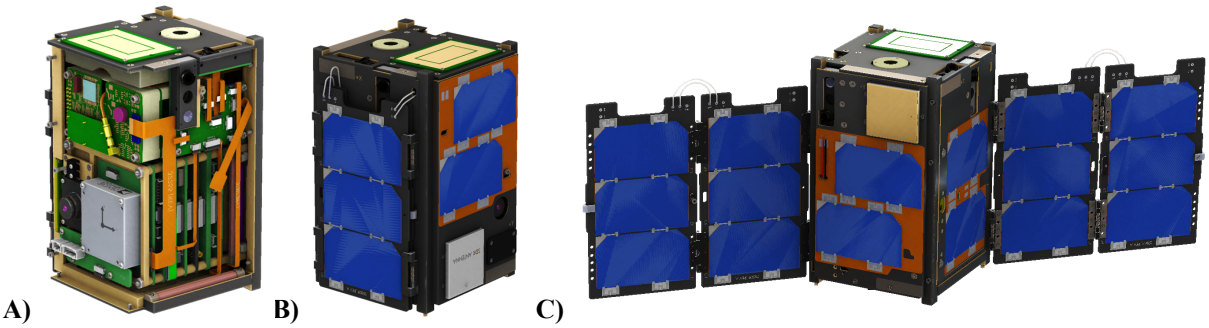

Figure 6: LLITED CubeSat shown as: A) a transparent model demonstrating subsystem/payload

Because of the power required to operate the payloads, maximizing power generation is a priority. This is achieved by utilizing next generation high efficiency solar cells and bi-fold solar panels. As mentioned previously, the bi-fold panels are unlike previous missions. They are a completely new design and were considered one of the most high-risk aspects of the project. Thus, design work began early in the project. Figure 7 shows a prototype panel and hinge mechanism in the a) closed and b) open state mounted to a test fixture. Panel deployment was extensively tested to ensure no break or degradation to the wires occurred. The panel will also be deployed in vacuum at the hot and cold limits.

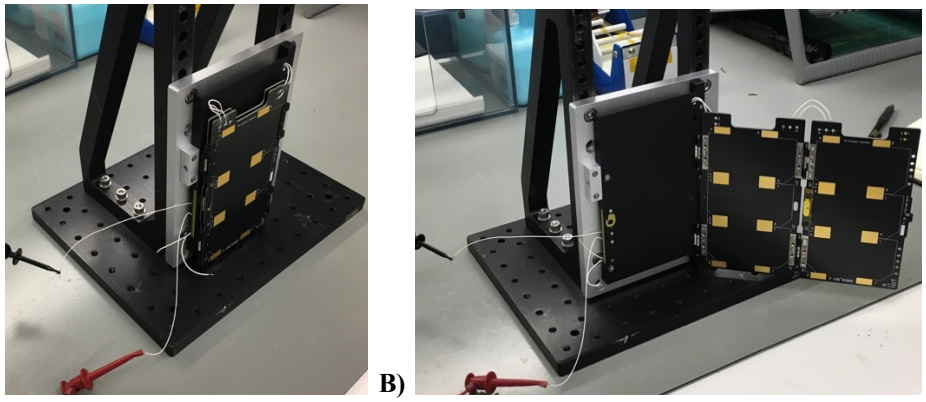

Figure 7: Prototype solar panel mounted in a test fixture A) stowed and B) deployed.

Payload Overview

Each of the two 1.5U CubeSats will host a miniature ionization gauge space instrument (MIGSI), planar ion probe (PIP), and GPS radio occultation sensor (CTECS-A). The Aerospace Corporation is providing the IG and CTECS-A sensors and Embry-Riddle is providing the PIP. The products provided are in-situ neutral pressure/density, in-situ plasma density, and slant TEC. The observations from LLITED will be combined with other available data, such as the remote sensing observations of ICON, to provide a comprehensive and compelling dataset of the ETWA. Table 2 shows the sensor performance and their relation to the science mission requirements.

Table 2: Mission Traceability

Parameter	Requirement	MIGSI	PIP	CTECS-A
Scientific Measurement	**Neutral Density, in-situ and Background Plasma Density**	**Pressure (Neutral Density)**	**Ion Density**	**TEC (also Ne)**
Instrument Performance	Precision: 10% (Nn, Ne); 3TECU	10^{-8} to 10^{-2} torr Precision: 0.1% Accuracy: 20% Sampling Rate: 1 Hz	$2x10^{9}$ to $2x10^{13}$ m^{-3} Sampling Rate 1Hz	3-200 TECU r.m.s. = 3 TECU
Heritage	---	LAICE CubeSat	DICE CubeSat, WADIS and MTeX rockets	Antenna: SENSE; Receiver: AC7-9
Current TRL		4	6	Antenna: 8, Receiver: 3
Horizontal Cell Size	15 km	Capability: 400 m, Mission Op.: 1km	Capability: 8 m; Mission Op.: 1km	N/A
Vertical Cell Size	N/A	N/A	N/A	~1 km
Attitude Requirements	As needed for sensors	Ram facing, 3-axis stable, 1° control, 0.1° knowledge	Ram facing, 3-axis stable, 10° control, 1° knowledge	Ram facing, 3-axis stable, 15° control
Field of View	As needed for sensors	180°	180°	180°
Voltage	Bus supplies +5 or +12V	+12V & +5V	+5V	+5V
Average Power	2.73 to 3.5 W (Payloads only)	3.57 W	0.25 W	1-1.3 W
Mass	0.6 kg	~200g	~220 g	~140g
Volume	0.5 U	Board: ~10 x 9 x 1 cm Chamber: ~6 cm spherical	Board: ~10 x 10 x 1cm Plate: 5 x 6 x 0.5 cm	Receiver: ~10 x 10 x 1 cm Antenna: 7.6x 7.6 x 1.3 cm
Duty Cycle	60% of orbit coverage	60% (2.14 W OAP)	60% (0.15 W OAP)	60% (0.78 W OAP)
Data Rate	115.2 kbps for each of four stations 2 contacts/day of minimum 3 min duration	Nominal: 256 bits/sec	48 bits/sec	Variable: 1000-1778 bits/sec

Miniature Ionization Gauge Space Instrument (MIGSI)

The Aerospace's Miniature Ionization Gauge Space Instrument consists of three components: Bayard-Alpert sensor, an accommodation chamber, and a controller. The sensor operates by measuring the pressure inside the accommodation chamber. The MIGSI aperture must be located on the ram face of the spacecraft to admit incoming neutral gas. An additional requirement is that the spacecraft is 3-axis stabilized and that the alignment of the aperture with the velocity vector is within 1°. MIGSI is a modified design based on The Aerospace Corporation's ionization gauge that flew successfully on the STREAK satellite mission.[24] The ionization gauge electronics has been adapted and delivered for a payload on the NSF LAICE CubeSat mission. For LLITED, the electronics has been split into two boards. Figure 8 shows the completed engineering unit. On top are the two electronics board (double-sided populated). The silver cylinder in the center is the ionization gauge itself (filament and collector) and the bottom gold sphere is the accommodation chamber.

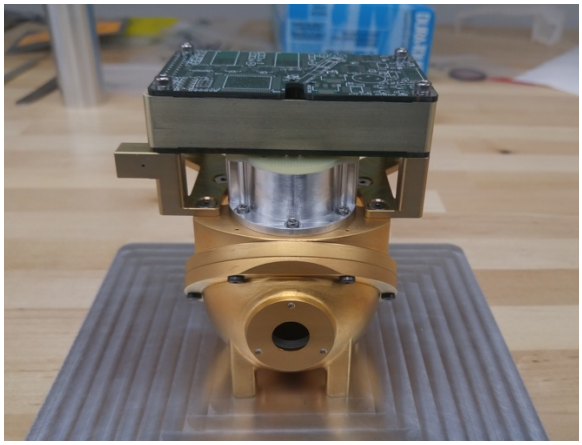

Figure 8: The assembled MIGSI engineering unit.

MIGSI will operate similar to the IGS flown on the STREAK mission. The amount of gas rammed into the sensor will be dependent on the vehicle velocity and orientation, and several parameters of the ambient gas. Using elementary gas kinetic theory and a set of simple assumptions, a fully general expression for the response of the instrument to the gas flow can be derived.[23] The assumptions are: the amount of gas entering the chamber is the same as that leaving, the sensor is operating in a free-molecular flow regime, and the gas measured by the gauge has been completely accommodated to the temperature of the chamber walls. Since the s/c speed through the medium is expected to be much greater than the thermal speed of the ambient gas, a simplified expression can be used with negligible loss of accuracy. The resulting equation is:

$$N_{meas} = \sqrt{\frac{\pi \overline{m}}{k_B T_{meas}}} n_{amb} v \quad (1)$$

where N_{meas} is the gas density in the accommodation chamber, T_{meas} the measured temperature of the chamber, n_{amb} is the ambient number density, m is the ambient molecular weight, and v is the "in-track" component of the s/c velocity through the ambient gas, and k_B is the Boltzman constant. MIGSI is sensitive to both changes in density and in-track winds. Thus, to aid in the interpretation of data LLITED requires a high inclination orbit so that MIGSI will primarily sense meridional winds.

Planar Ion Probe (PIP)

Langmuir probes have been routinely used on sounding rockets and satellites to measure in-situ plasma density.[25,26] They can be implemented as fixed bias (DC) probes or can have their bias swept from negative to positive potential with respect to s/c chassis ground. Swept bias probes provide absolute plasma density and electron temperature with every sweep, but require the spacecraft surface to probe area ratio to be above 10000.[27] If this area ratio is smaller, as it usually is for rockets and CubeSats, then the sweeping bias on the Langmuir probes swings the floating potential of the spacecraft thereby "warping" the applied potential, which can be detrimental to other electrical probes onboard.[28] Fixed bias Langmuir probes measure the collected current at a fixed potential either in the electron saturation region or the ion saturation region. The current in the saturation regions is directly proportional to plasma density. For cylindrical and spherical probes, the collection current changes with applied bias with respect to the plasma potential, and the applied bias can change with spacecraft floating potential changes, which varies with electron temperature. On the other hand, planar probes (Planar Ion/Electron Probe) have a flat current collection characteristic in the saturation regions. Thus, small changes in applied bias due to the fluctuating floating potential have no impact on the saturation region collection current. Furthermore, at orbital velocities the ram collection current for ions is about 10 times as high as the thermal ion current. Since the orbital velocity and the ram cross section of the planar probe are known, the ion ram current riding on top of the ion saturation current becomes a very good and simple measurement of the absolute ion density.

Using a Planar Ion Probe (PIP) requires that the probe be located on the ram face of a 3-axis controlled s/c. This technique is also well tolerant of pointing errors as long as: (a) the pointing deviation from ram direction is known to correctly account for ram cross section of the probe surface, (b) the off pointing is not so high that it reduces the collected current into the instrument noise. Typically, a 10° pointing error is well tolerated along with 1° pointing knowledge.

The LLITED PIP is (4 x 6 cm rectangle) with a guard band that is 1 cm wide with a 1 mm gap between the probe surface and the guard. The PIP will be fixed biased at -7 V relative to CubeSat chassis (ion saturation region) and placed on the ram facing surface. Operating in the ion saturation region leads to smaller current collection from the plasma resulting in less spacecraft charging. This is essential to guarantee proper functionality of the ionization gauge.

In the spring of 2019, an assembled PIP engineering unit successfully completed vibrational testing. Figure 9 shows the electronics board and the gold-plated collection plate. PIP has a measurement range of $2x10^9$ to $2x10^{13}$ m^{-3} with a resolution of $2x10^8$ m^{-3}. Oversampling and decimation of the resultant signal will be done between the distinct telemetry sample points to improve the signal to noise. The current instrument is capable of any desired sample rate not exceeding 150 Hz but the nominal rate for LLITED is 100 Hz. The noise floor resolution is $3.13x10^8$ m^{-3} and ~$7.0x10^7$ m^{-3} for low and high gain, respectively. It has 10% precision through the four decades of measurement.

The probe electronics have heritage from the NSF Dynamic Ionosphere CubeSat Experiment (DICE) on which Dr. Barjatya was the instrument PI for the Langmuir probes, as well as the recently launched DLR WADIS rockets and NASA Mesospheric Turbulence Experiment (MTeX) sounding rockets on which Dr. Barjatya provided a suite of Langmuir probes.[29]

A) 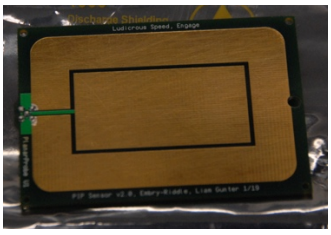 B) 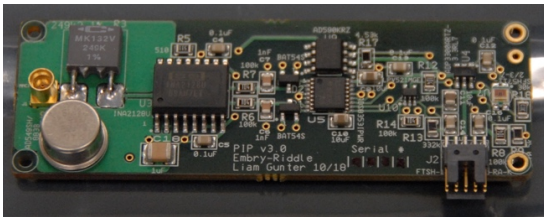

Figure 8: The completed PIP engineering unit with A) collector plate and B) electronics board.

Compact Total Electron Content Sensor – Aerospace (CTECS-A)

The Space Science Application Laboratory at The Aerospace Corporation has extensive experience with GPS science sensors dedicated to radio occultation measurements of the ionosphere, as well as CubeSat GPS navigation receivers. Our first science sensor, the Ionosphere Occultation Experiment (IOX) on PicoSat-9, operated from 2001-2004.[30] The second was the C/NOFS Occultation Receiver for Ionospheric Sensing and Specification (CORISS) part of the C/NOFS mission from 2008 to 2015.[31] Both the IOX and CORISS receivers were JPL BlackJack receivers. In 2011, we developed the Compact Total Electron Content Sensor (CTECS) for CubeSat and nanosat platforms using NovAtel commercial receivers. CTECS successfully collected science data on the PSSCT-2 mission in 2011 and SENSE mission in 2013-2015.[32]

In parallel, the Aerospace's Digital Communication Implementation Department developed a single frequency (L1) GPS receiver for position/navigation/timing (PNT) for use on CubeSats. The receiver is based on a terrestrial software defined radio that was ported for space applications. Unlike MIGSI and PIP, the GPS receiver is an integrated part of the CubeSat bus. The receiver is part of the Flight, GPS, Attitude control (FGA) board. Because of this unique situation, it is treated as a subsystem rather than a payload. This is continued for the expanded receiver CTECS-A on LLITED.

The CTECS–A is a GPS sensor for small satellites that provides PNT and can be used for either overhead or occulting science observations. CTECS-A consists of a custom GPS receiver (including the RF front end) and a custom antenna (Figure 9). On previous Aerospace CubeSat missions that carried CTECS, an additional Aerospace single frequency GPS receiver was also flown for navigation since it was part of the standard Aerospace CubeSat bus designs. Unlike earlier versions of CTECS that used NovAtel receivers, CTECS-A uses an expanded version of The Aerospace Corporation's PNT CubeSat receiver. Thus, eliminating the need for two receivers and freeing space within the bus. Currently the Aerospace receiver is single frequency (L1), has 10 channels, and provides an accuracy of 10-20 m (without ionospheric corrections). For LLITED, the Aerospace receiver will be upgraded to include GPS L2 (P(Y) and C) tracking, computation and output of pseudorange and Accumulated Doppler Range (ADR, i.e. phase) for both L1/L2 frequencies, increased number of channels to track 12 dual frequency satellites, and improved position accuracy. Table 2 provides the expected SWAP of the receiver and power.

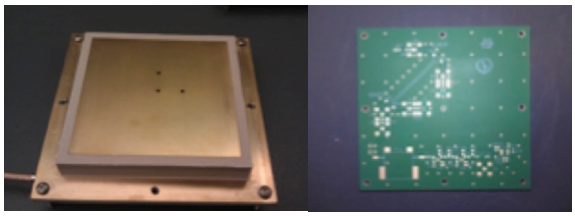

Figure 9: The front/back SENSE CTECS custom antenna. CTECS-A will use the same antenna.

The range of TEC measured is 3-200 TECU. CTECS-A is also capable of providing scintillation (S4) observations within the range of 0.1 to 1.5 with an uncertainty of 0.1. The data rate is variable depending on the number of satellites tracked and the sampling rate. For previous CTECS sensors utilizing the NovAtel receiver, the data rate averaged 1778 bits/sec (800 kB/hour), which is the baseline for CTECS-A.

Mission Orbit and Operations

The LLITED mission has been selected by NASA's CubeSat Launch Initiative. LLITED requests a circular orbit between 400-500 km but with 450 km preferred. The inclination should be between 70° and 110°. Upon release, the satellite powers up in its lowest power mode, without ACS, and is therefore tumbling. It has been designed to survive (RF antenna pattern, thermal and power) in this safe mode. Within the first 6 hours, the satellite will fly over one of Aerospace's ground stations. Contact will be made

and the state-of-health telemetry records downloaded. If the satellite is nominal, then on the next contact the wings on CubeSat A will be opened and the differential drag will start to separate one satellite from the other. Checkout of the attitude control system and payloads will be performed during this separation phase. After 1- month of separation, the satellites will be 180° in phase and the wings on satellite B will be opened. At this time, both vehicles will be ready to start mission operations.

Embry-Riddle has developed a capability to optically track and characterize resident space objects as small as 1U CubeSats [33]. The effort was a result of an NSF grant and captured videos and photometry of satellites can be seen at sail.erau.edu/OSCOM.html. As a result of this tracking, it is possible to: (a) confirm and refine the TLE of CubeSats, (b) retrieve spin/tumble rate, (c) determine the status of deployables, and (d) identify individual satellites in a constellation. The capability has recently been enhanced to do multipoint simultaneous tracking and thus it is now possible to deduce crude attitude estimates. Such optical information is crucial for an operational satellite and is indispensable for anomaly analysis. LLITED will use this technique in order to provide confirmation of the deployment and orientation of the two s/c.

Nominal operations consist of the two CubeSats in LVLH (3-axis stabilized) between ±45° latitude to perform science operations. At higher latitudes, the s/c will perform a maneuver to obtain a sun-pointing orientation to maximize power collection. As the s/c enters the science operations latitude, it will return to LVLH. Figure 10 illustrates the proposed maneuvers.

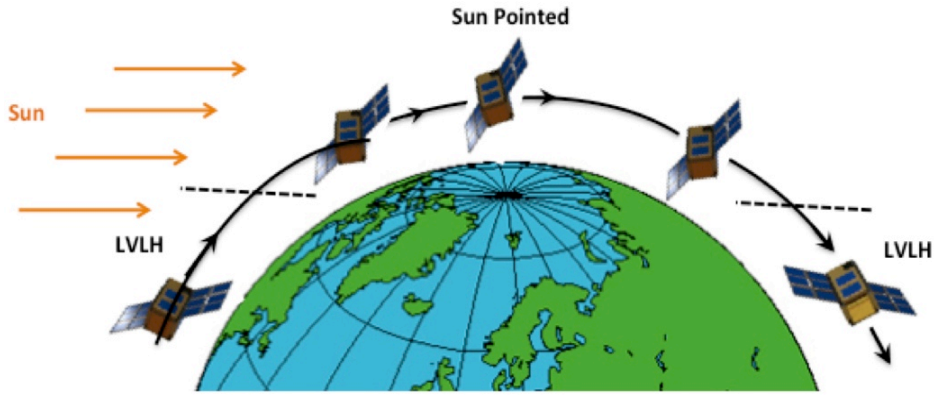

Figure 10: Illustration of operational mode maneuver. The s/c will be sun-pointed for latitudes > |60°| latitude to maximize power collection.

Ground-System

The LLITED satellites will utilize The Aerospace Corporation's proven half-duplex 915 MHz ADV Radio architecture. To support this radio, Aerospace has developed a network of five automated ground stations dedicated to PicoSats that are spaced across the United States in order to increase connectivity and downlink. These stations are used to command and monitor the satellite and down link the science data. Currently, three ground-stations are on-line: Texas A&M, University of Florida, and Hawaii. A fourth station located at Vandenberg, AFB has been installed and will be online later this year.The ground stations are automated 2-meter diameter parabolic dishes operating at 915MHz with a downlink rate of 115.2 kbps. The automated stations allow the mission manager, located at The Aerospace Corporation in El Segundo, CA, to enter a list of desired commands, their execution times, and the data to be down-linked into a central computer along with a summary report. The five stations combined provide a nominal data download of ~25 MB per day, assuming two contacts per day with a minimum three-minute duration.

CURRENT STATUS

The Project Initiation Management Review, required at the beginning of any hardware project at The Aerospace Corporation, occurred in late September 2017 followed by a team kickoff meeting in early October 2017. The System Requirements Review (SRR) occurred in March 2018. Because LLITED is a fixed grant, a different strategy was adopted. First, instead of a traditional preliminary and critical design

review (PDR/CDR) for the entire LLITED spacecraft, individual design reviews and then a final Design Review (DR) was planned. Second, it was decided that payload development would lead bus development with the exception of new boards and subsystems, which would begin immediately in order to burn-down risk to the project. These include the payload interface and high voltage daughter board, and bifold wings. Effort was limited to the payloads and the listed subsystems for the first 9 months. In-depth design reviews for each payload was completed prior to beginning flight hardware. This resulted in completed MIGSI and PIP engineering units, and bi-fold wing and payload interface board prototypes in early 2019. Starting in spring of 2019, design of the bus began in earnest. At this point AeroCube-10 has been delivered and LLITED is able to take advantage of the latest subsystem designs. For several months, individual in-depth peer reviews of each subsystem board occurred culminating in a Design Review in June 2019.

SUMMARY

The Low-Latitude Ionosphere/Thermosphere Enhancements in Density (LLITED) CubeSat mission will provide ionosphere and thermosphere measurements to increase our knowledge of the duskside dynamics that may influence space weather. Two 1.5U CubeSats in a high-inclination circular orbit, with an orbit altitude between 400 and 500 km will make measurements related to the Equatorial Ionization Anomaly (EIA) and the Equatorial Temperature and Wind Anomaly (ETWA). The Aerospace Corporation will design and build the CubeSats that will host three payloads to obtain measurements of in-situ thermospheric density and plasma density, and background TEC. The instruments are an ionization gauge (MIGSI), planar ion probe (PIP), and GPS radio occultation sensor (CTECS-A).

Acknowledgments

This work is supported by NASA Grant 80NSSC17K0044.

References

1. Namba, S., and K.I. Maeda, Radio wave propagation, p. 86, Corona, Tokyo, 1939.
2. Abdu, M.A., G.O. Walker, R.M. Reddy, E.R. de Paula, J.H.A. Sobral, B.G. Fejer, “Global Scale Equatorial Ionization Anomaly (EIA) Response to Magnetospheric Disturbances Based on the May-June 1987 SUNDIAL-Coordinated Observations”, Annales of Geophysicae, vol. 11, No. 7, 1993.
3. Basu, S., S. Basu, J. Huba, J. Krall, S.E. McDonald, J.J. Makela, E.S. Miller, S. Ray, K. Groves, “Day-to-Day Variability of the Equatorial Ionization Anomaly and Scintillations at Dusk Observed by GUVI and Modeling by SAMI3,” Journal of Geophysical Research, 114, A04302, http://dx.doi.org/10.1029/2008JA013899, 2009.
4. Yue, X., W.S. Schreiner, Y.-H. Kuo, J. Lei, “Ionosphere Equatorial Ionization Anomaly Observed by GPS Radio Occultations During 2006-2014,” Journal of Atmosphere and Solar Terrestrial Physics, vol. 129, doi:10.1016/j.jastp.2015.04.004, 2015.
5. Philbrick, C.R., and J.P. McIsaac “Measurements of Atmospheric Composition Near 400 km”, Space Research XII, 1972.
6. Raghavarao, R., and R. Suhasini, “Equatorial Temperature and Wind Anomaly (ETWA) – A Review, Journal of Atmosphere and Solar Terrestrial Physics, vol. 64, 2002.
7. Hedin, A.E., and H.G. Mayr 1973, “Magnetic Control of the Near Equatorial Neutral Thermosphere”, Journal of Geophysical Research, vol. 78, No. 10, doi:10.1029/JA078i010p01688, 1973.
8. Fuller-Rowell, T., M. Codrescu, B. Fejer, W. Borer, F. Marcos, D. Anderson, “Dynamics of the Low-Latitude Thermosphere: Quiet and Disturbed Conditions”, Journal of Atmosphere Solar Terrestrial Physics, vol. 59, No. 13, doi:10.1016/S1364-6826(96)00154-X, 1977.
9. Pant, T.K., and R. Sridharan, “Plausible Explanation for the Equatorial Temperature and Wind Anomaly (ETWA) Based on Chemical and Dynamical Processes”, Journal of Atmosphere Solar Terrestrial Physics, vol. 63, No. 9, doi:10.1016/S1364-6826(00)00196-6, 2001.
10. Miyoshi, Y., H. Fujiwara, H. Jin, H. Shinagawa, H. Liu, K. Terada, “Model Study on the Formation of the Equatorial Mass Density Anomaly in the Thermosphere” Journal of Geophysical Research, vol. 116, No. A05322, doi:10.1029/2010JA016315, 2011.
11. Lei, J., J.P. Thayer, W. Wang, A.D. Richmond, R. Roble, X. Luan, X. Dou, X. Xue, T. Li, “Simulations of the Equatorial Thermosphere

Anomaly: Field-aligned Ion Drag Effect", Journal of Geophysical Research, vol. 117, No. A01304, doi:10.1029/2011JA017114, 2014.

12. Maruyama, N., S. Watanabe, T.J. Fuller-Rowell, "Dynamic and Energetic Coupling in the Equatorial Ionosphere and Thermosphere", Journal of Geophysical Research, vol. 108, No. A11, 1396, doi:10.1029/2002JA009599, 2003.
13. Lei, J., J.P. Thayer, W. Wang, J. Yue, X. Dou, "Nonmigrating Tidal Modulation of the Equatorial Thermosphere and Ionosphere Anomaly", Journal of Geophysical Research: Space Physics, 119, 3036–3043, doi:10.1002/2013JA019749, 2014.
14. Lei, J., W. Wang, J.P. Thayer, X. Luan, X. Dou, A.G. Burns, and S.C. Solomon, "Simulations of the Equatorial Thermosphere Anomaly: Geomagnetic Activity Modulation", Journal of Geophysical Research: Space Physics, vol. 119, doi:10.1002/2014JA020152, 2012.
15. Hsu, V. W, J. P. Thayer, L. Lel, and W. Wang, "Formation of the Equatorial Thermosphere Anomaly Trough: Local Time and Solar Cycle Variations, Journal of Geophysical Research: Space Physics, vol. *119*, doi:10.1002/2014JA020416, 2014.
16. Lei, J., J.P. Thayer, W. Wang, X. Luan, X. Dou, and R. Roble, "Simulations of the Equatorial Thermosphere Anomaly: Physical Mechanisms for Crest Formation", Journal of Geophysical Research, vol. 117, No. A06318, doi:10.1029/2012JA017613, 2012.
17. Lei, J., J.P. Thayer, J.M. Forbes, "Longitudinal and Geomagnetic Activity Modulation of the Equatorial Thermosphere Anomaly", Journal of Geophysical Research, vol. 115, No. A08311, doi:10.1029/2009JA015177, 2010.
18. Luan, X., P. Wang, X. Dou, and Y.C.-M. Liu, "Interhemispheric Asymmetry of the Equatorial Ionization Anomaly in Solstices Observed by COSMIC During 2007–2012", Journal Geophysical Research: Space Physics, vol. 120, doi:10.1002/2014JA020820, 2015.
19. Clemmons, J.H., R.L. Walterscheid, A.B. Christensen, and R.L. Bishop, "Rapid, highly structured meridional winds and their modulation by non-migrating tides: Measurements from the Streak mission", Journal of Geophysical Research, vol. 118, No. 2, doi:10.1029/2012JA017661, 2013.
20. Picone, J.M., A.E. Hedin, D.P. Drob, and A.C. Aikin, "NRLMSISE-00 Empirical Model of the Atmosphere: Statistical Comparisons and Scientific Issues", Journal Geophysical Research., vol. 107, doi:10.1029/2002JA009430, 2002.
21. Zhang, Y., L.J. Paxton, H. Kil, "Nightside Midlatitude Ionospheric Arcs: TIMED/GUVI Observations", Journal of Geophysical Research: Space Physics, vol. 118, No. 6, doi:10.1002/jgra.50327, 2013.
22. Raghavarao, R., W.R. Hoegy, N.W. Spencer, L.E. Wharton, "Neutral Temperature Anomaly in the Equatorial Thermosphere – A Source of Vertical Winds", Geophysical Research Letters, vol. 20, 1993.
23. Horowitz, R., and H.E. LaGow, "Upper Air Pressure and Density Measurements From 90 to 220 Kilometers with the Viking 7 Rocket", Journal Geophysical Research, vol. 62, 1957.
24. Clemmons, J.H., L.M. Friesen, N. Katz, M. Ben-Ami, Y. Dotan, R.L. Bishop, "The Ionization Gauge Investigation for the Streak Mission", Space Science Reviews, vol. 145, No. 3-4, doi:10.1007/s11214-009-9489-6, 2009.
25. Brace, L. H., "Langmuir Probe Measurements in the Ionosphere, Measurement Techniques in Space Plasmas: Particles", ser. Geophysical Monograph Series, *ed. R. F. Pfaff et al.*, Ed. Washington D. C.: American Geophysical Union, vol. 102, 1998
26. Barjatya A., C.M. Swenson, D.C. Thompson, and K.H. Wright, Jr., "Data Analysis of the Floating Potential Measurement Unit aboard the International Space Station", Review of Science Instrumentation, doi:10.1063/1.3116085, 2009.
27. Szuszczewicz, E. P., Area Influences and Floating Potentials in Langmuir Probe Measurements", Journal of Applied Physics, vol. 43, No. 3, 1972.
28. Barjatya A., J.P. St. Maurice, and C.M. Swenson, "Elevated Electron Temperatures Around Twin Sporadic E Layers at Low Latitude: Observations and the Case for a Plausible Link to Currents Parallel to the Geomagnetic Field", Journal of Geophysical Research, vol. 118, doi:10.1002/2013JA018788, 2013.
29. Fish, C.S., C.M. Swenson, G. Crowley, A. Barjatya, T. Neilsen, J. Gunther, I. Azeem, M. Pilinski, R. Wilder, D. Allen, M. Anderson, B. Bingham, K. Bradford, S. Burr, R. Burt, B. Byers, J. Cook, K. Davis, C. Frazier, S. Grover, G. Hansen, S. Jensen, R. LeBaron, J.

Martineau, J. Miller, J. Nelsen, W. Nelson, P. Patterson, E. Stromberg, J. Tran, S. Wassom, C. Weston, M. Whiteley, Q. Young, J. Petersen, S. Schaire, C. R. Davis, M. Bokaie, R. Fullmer, R. Baktur, J. Sojka, M. Cousins, "Design, Development, Implementation, and On Orbit Performance of the Dynamic Ionosphere CubeSat Experiment Mission", Space Science Review, vol. 181, No. 1-4, 2014.

30. Straus, P.R., "Ionospheric Climatology Derived From GPS Occultation Observations Made by the Ionospheric Occultation Experiment", Advances in Space Research, vol. 39, No. 5, doi:10.1016/j.asr.2006.08.009, 2007.

31. de La Beaujardiere, O., "C/NOFS: A Mission to Forecast Scintillation", Journal of Atmosphere Solar Terrestrial Physics, vol. 66, doi:10.1016/j.jast.2004.07.030, 2004.

32. Bishop, R. L., D.A. Hinkley, D.R. Stoffel, D. E. Ping, P.R. Straus, and T.R. Brubaker, "First Results from the GPS Compact Total Electron Content Sensor (CTECS) on the PSSC-2 Nanosat", Proceedings of the 26th Annual AIAA/USUS Conference of Small Satellites, SSC12-XI-2, 2012.

33. Gasdia, F, A. Barjatya and S. Bilardi, "Multi-site simultaneous time-resolved photometry with a low cost electro-optics system", Sensors 2017, 17(6), 1239; doi:10.3390/s17061239.